

ORIGINAL RESEARCH ARTICLE

Network pharmacology and bioinformatics reveal the multi-target mechanisms of the Qiang-gu-jian-shen formula osteoporosis treatment

 Cuicui Zhou^{1,2}, Zarina Awang¹, and Farra Aidah Jumuddin^{1*}
¹Department of Clinical Medicine, Faculty of Medicine, Lincoln University College, Petaling Jaya, Selangor, Malaysia

²Department of Orthopaedic Surgery, The Second Affiliated Hospital of Nanyang Medical College, Nanyang, Henan, China

Abstract

Osteoporosis (OP) is a systemic skeletal disease characterized by reduced bone mass and deteriorated bone microstructure, significantly increasing fracture risk. As global aging intensifies, OP has become a significant public health issue. Present pharmacological interventions, such as bisphosphonates and selective estrogen receptor modulators, are associated with side effects and limitations, highlighting the need for safe and effective alternatives. This study investigates the potential mechanisms of the Qiang-gu-jian-shen formula (QGJSF), a traditional Chinese medicine (TCM) compound, in treating OP using network pharmacology and bioinformatics. A total of 1,395 potential targets for QGJSF were identified by querying the TCMSP and BATMAN-TCM databases and converting targets through UniProt. Cross-referencing with OP-related targets from GeneCards, OMIM, and DisGeNET yielded 500 mapped targets. Protein-protein interaction network constructed through the STRING database led to the identification of 69 core targets. An “herb-active component-target” network was built using Cytoscape 3.9.0. Gene ontology functional annotation and Kyoto Encyclopedia of Genes and Genomes pathway enrichment analyses highlighted key pathways, including the PI3K/AKT and FoxO. Molecular docking showed that key components, such as quercetin, dioscin, genistein, calycosin, and berberine, bind favorably to core targets (binding energies < -5 kcal/mol). GEO dataset (GSE5958) analysis identified seven common core genes, including *TGFB1*, *MMP2*, *BCL2L1*, *MAPK3*, *AKT1*, *CTNNA1*, and *TP53*. The findings suggest that QGJSF may improve OP through multiple components that regulate osteoblast differentiation, osteoclastogenesis, and activate key pathways, such as Wnt/ β -catenin, PI3K/AKT, and JAK/STAT, thereby enhancing bone formation and reducing resorption. Core targets such as ESR1, STAT3, AKT1, and TP53 regulate bone metabolism by modulating osteoblasts, osteoclasts, and their interactions with immune and hematopoietic cells to maintain bone remodeling. This study advances understanding of QGJSF’s mechanisms and provides a foundation for novel OP therapies. Future validation and exploration of additional therapeutic targets and mechanisms are needed.

Keywords: Qiang-gu-jian-shen formula; Osteoporosis; Network pharmacology; Mechanisms

*Corresponding author:

 Farra Aidah Jumuddin
 (farraaidah@lincoln.edu.my)

Citation: Zhou C, Awang Z, Jumuddin FA. Network pharmacology and bioinformatics reveal the multi-target mechanisms of Qiang-gu-jian-shen formula osteoporosis treatment. *Eurasian J Med Oncol.* 2025;9(2):270-284. doi: 10.36922/EJMO025150103

Received: April 10, 2025

Revised: May 13, 2025

Accepted: May 14, 2025

Published online: June 18, 2025

Copyright: © 2025 Author(s). This is an Open-Access article distributed under the terms of the Creative Commons Attribution License, permitting distribution, and reproduction in any medium, provided the original work is properly cited.

Publisher’s Note: AccScience Publishing remains neutral with regard to jurisdictional claims in published maps and institutional affiliations.

1. Introduction

Osteoporosis (OP) is a systemic skeletal disease characterized by reduced bone mass and degeneration of bone microstructure, which significantly increases the risk of fractures and severely affects patients' quality of life and life expectancy. With the acceleration of global population aging, OP has become an important public health challenge. According to data from the International OP Foundation, over 200 million people worldwide were affected by OP as of 2020, with an OP-induced fracture occurring approximately every 3 s. Since 1990, the global incidence of hip fracture has steadily increased, with projections estimating a 240% rise among women and a 310% increase among men by 2050. Furthermore, approximately 50% of individuals who experience osteoporotic fractures are likely to suffer a subsequent fracture.^{1,2}

Clearly, as the degree of global population aging deepens further, the incidence of OP has risen to become the third most common chronic disease following cardiovascular diseases and diabetes, becoming one of the ten important chronic diseases threatening human health. Traditional treatment methods mainly rely on pharmacological interventions, such as bisphosphonates and selective estrogen receptor modulators. However, these treatments come with certain side effects and limitations, including gastrointestinal discomfort and kidney damage, especially with prolonged use.³ Therefore, the exploration of safe and effective alternative therapies is essential.

In recent years, traditional Chinese medicine (TCM) formulas have received considerable attention for their application in preventing and treating OP. Due to their multi-target and multi-level mechanisms of action, TCM has shown unique advantages in improving bone metabolism and enhancing bone density.⁴ The Qiang-gu-jian-shen formula (QGJSF) is composed of six medicinal herbs, including Cortex Eucommiae (Du Zhong, DZ), Fructus Lycii (Gou Qi, GQ), Radix Achyranthis Bidentatae (Niu Xi, NX), Radix Astragali (Huang Qi, HQ), Chuanxiong Rhizoma (Chuanxiong, CX) and Rehmanniae Radix Praeparata (Shu Di Huang, SDH), has demonstrated significant efficacy in clinical treatments for OP. Based on TCM principles that "the kidneys govern the bones" and "the liver and kidneys share a common origin," QGJSF aims to replenish kidneys and essence, promote blood circulation, resolve stasis, and strengthen muscles and bones. Although its clinical success, the specific mechanisms of action underlying QGJSF have not been fully elucidated.

In recent years, the development of systems biology has brought new perspectives for studying complex diseases by enabling the integration of multi-omics data to facilitate a deeper understanding of disease mechanisms.

In the field of TCM research, network pharmacology has emerged as a novel methodology. By merging techniques from systems biology, bioinformatics, and computational chemistry, network pharmacology allows for a holistic elucidation of the mechanisms of action of TCM formulas. Previous studies utilizing network pharmacology have made progress in deciphering the mechanisms of TCM compound formulas. However, limitations remain, such as limited depth in target-disease association analyses and a lack of comprehensive analysis across multiple databases.⁵⁻⁷

This study employs integrated network pharmacology and bioinformatics approach to systematically investigate the multidimensional therapeutic mechanism of the QGJSF against OP. The active components in QGJSF and their potential targets were identified using the TCMSP and BATMAN-TCM databases, while OP-related targets were retrieved from GeneCards, OMIM, and DisGeNET databases. A compound-disease target interaction network was constructed using the bioinformatics platform, followed by a protein-protein interaction (PPI) network through the STRING database. Core therapeutic targets were identified through topological analysis through Cytoscape. Functional annotation through the DAVID database facilitated comprehensive gene ontology (GO) and Kyoto Encyclopedia of Genes and Genomes (KEGG) pathway enrichment analyses, elucidating key biological processes (BP) and signaling pathways involved in the anti-osteoporotic effects of QGJSF. Molecular docking using AutoDock tools validated binding affinities between bioactive components and core targets, while GEO database-derived clinical data verification and gene set enrichment analysis (GSEA) further deciphered the regulatory networks of pivotal genes. Overall, this study offers scientific evidence supporting the multi-component, multi-target, multi-pathway mechanisms underlying QGJSF's therapeutic efficacy against OP and establishes an innovative methodological framework for modernizing TCM formulations through systems biology approaches.

2. Materials and methods

2.1. Screening for targets related to QGJSF

Targets associated with QGJSF were identified through searches using the TCMSP (<https://old.tcmisp-e.com/disease.php?qd=421>) and BATMAN-TCM (<http://bionet.ncpsb.org/batman-tcm/>) databases. The identified targets were converted using the UniProt database, and duplicate entries were removed. For TCMSP data, targets were screened using criteria of oral bioavailability $\geq 30\%$ and drug-likeness ≥ 0.18 . In the BATMAN-TCM database, screening was based on a score cutoff of 0.84, an adjusted *p*-value (Benjamin-Hochberg correction) ≤ 0.05 , and

druggable score ≥ 0.1 . Targets obtained from both databases were combined, and duplicate entries were removed to ultimately acquire the potential targets of the QGJSF.

2.2. Acquisition of OP Targets

Disease targets related to OP were retrieved by searching the GeneCards (<https://www.genecards.org/>), OMIM (<https://omim.org/>), and DisGeNET (<https://disgenet.com/>) databases using “osteoporosis” as the search term.

2.3. Construction of PPI network for key targets of QGJSF in treating OP

Targets related to the treatment of OP by QGJSF were uploaded to the online platform Wei Sheng Xin website (<https://www.bioinformatics.com.cn/>). Using the interactive Venn diagram tool, the intersection between QGJSF-associated targets and OP-related molecules was identified, which represents the potential targets of QGJSF for OP. These potential targets were then submitted to the STRING database (Version: 11.0, <https://string-db.org/>) for PPI analysis, with the species limited to *Homo sapiens* and the confidence score threshold set to the highest level (0.900), excluding isolated nodes.

2.4. Screening for core targets

The mapped targets obtained from the screening process were imported into the STRING database (<https://cn.string-db.org/>) to acquire the TSV file of the PPI network. This file was then imported into Cytoscape 3.9.0 software, and network analysis was performed using the Centiscape 2.2 plugin. The significance of each potential target was evaluated across three centrality measures: Degree, betweenness, and closeness. The intersection of the top-ranking targets was identified as the core targets, which were subsequently visualized for further analysis.

2.5. Construction of the “Drug-Target-Disease” network

The core targets associated with the treatment of OP by QGJSF were organized and imported into Cytoscape 3.9.0 to construct a “TCM-Active Component-Target” network, which was subsequently visualized for further analysis.

2.6. GO Function and KEGG Pathway Enrichment Analysis of Core Targets

GO functional annotation and KEGG pathway enrichment analysis were performed on the core targets through the DAVID database (Version: 6.8, <https://david.ncifcrf.gov/>), with both species and background set to *Homo sapiens*. The top 20 primary BP and non-disease, non-cancer-related signaling pathways with pharmacological relevance ($p < 0.05$) were selected to explore the potential mechanisms by which QGJSF may treat OP.

2.7. Molecular docking

Molecular docking was used to evaluate the binding affinity between active ingredients and their target proteins. The 3D structures of key active components from the QGJSF were downloaded from the PubChem database, and the 3D structures of core target proteins were obtained from the Protein Data Bank (PDB) (<https://www.rcsb.org/>). Protein receptors were pre-processed using PyMOL software to remove water molecules and ligands. Subsequently, the key components and target proteins were imported into AutoDockTools 1.5.7 for hydrogen atom addition and active site determination. The docking binding energy was then calculated. A binding energy of < 0 kcal/mol indicates that the receptor and ligand can bind spontaneously, while a binding energy < -5 kcal/mol suggests favorable binding activity.

2.8. GEO database validation

The “limma” R package was used to analyze the differential gene expression in the OP dataset GSE5958 from the GEO database (<https://www.ncbi.nlm.nih.gov/geo/>). Genes meeting the criteria of $|\log FC| > 1$ and an adjusted $p < 0.05$ were considered significant differentially expressed. Volcano plots and heatmaps were generated using the “ggplot2” and “pheatmap” R packages, respectively. A Venn diagram was utilized to identify common targets between the potential targets of *Strychni Semen* and the GSE5958 dataset. The expression of core genes was visualized and validated using dataset GSE35958 with the “ggpubr” package. Subsequently, receiver operating characteristic (ROC) curves were constructed using the “pROC” package to evaluate the predictive performance of marker genes.

2.9. GSEA

In this study, single-gene GSEA analysis was conducted using the “gseaplot2” package to investigate the potential functional role of the identified hub gene.

3. Results

3.1. Screening of targets related to QGJSF

The targets related to the QGJSF were retrieved from TCMSP and BATMAN-TCM databases. The identified targets were converted using the UniProt database, and duplicate entries were removed, resulting in a total of 1,395 potential targets for the QGJSF.

3.2. Acquisition of OP-related targets and common targets between drug and disease

A total of 2,784 OP-related targets were obtained from the GeneCards, OMIM, and DisGeNET databases. By intersecting the predicted targets of the QGJSF with

OP-related disease targets, a total of 500 mapped targets were identified, as shown in Figure 1.

3.3. Construction and analysis of the PPI network

A target PPI network was constructed using the STRING database with the association score (combined_score) threshold set at 0.9, and isolated nodes were excluded. In this network, nodes represent target proteins, while edges indicate associations between them. As shown in Figure 2, the PPI network contains 487 interconnected nodes and 1,896 edges, with an average node degree of 7.79 and an average local clustering coefficient of 0.421. The expected number of edges was 610, and the *p*-value for PPI enrichment was $<1.0e - 16$.

3.4. Topological analysis of the PPI network and selection of core targets

Topological parameters of the network, including betweenness centrality, closeness centrality, and degree centrality, were calculated for each node using the CentiScape 2.2 plugin. Based on these metrics, 33 core targets were selected and subsequently visualized, as shown in Figure 3.

3.5. Construction of “herb-active component-target” network

The key targets of QGJSF for the treatment of OP were organized and imported into Cytoscape 3.9.0 to construct an “herb-active component-target” network. The results were visually processed, as detailed in Figure 4. Based on degree values, the top 10 components were selected as the core active components in the treatment of OP using QGJSF. Combining these findings with relevant literature, five key active components were identified and are listed in Table 1.

3.6. GO function and KEGG pathway enrichment analysis

The target genes identified from the potent bone-strengthening and kidney-nourishing formula for OP treatment were imported into the DAVID database for enrichment analysis, with a screening threshold set at $p \leq 0.01$. The results were selected in ascending order by *p*-value, where a smaller *p*-value indicates a higher degree of enrichment. GO function enrichment analysis categorized the gene functions into three main categories, including BP, cellular component (CC), and molecular function (MF). A total of 2,073 GO terms were identified, including 1,637 BP entries, 149 CC entries, and 287 MF entries. The top 10 terms from each category were selected and visualized in GO analysis charts using MicroSignal (Figure 5A).

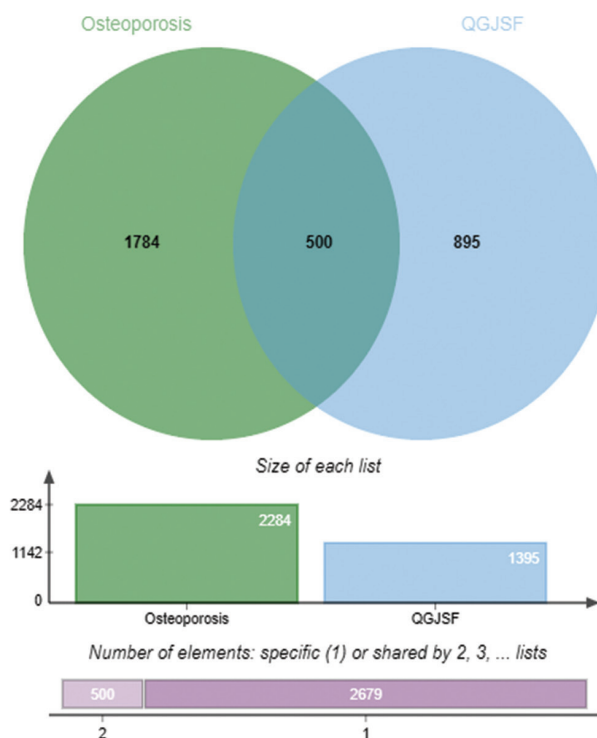


Figure 1. Acquisition of OP-related targets and common targets between drug and disease

Abbreviations: OP: Osteoporosis; QGJSF: Qiang-gu-jian-shen formula.

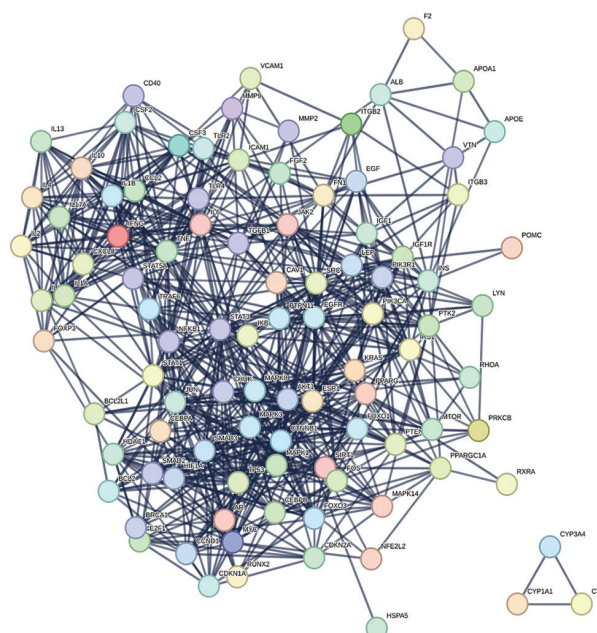


Figure 2. Potential target PPI network diagram

Abbreviation: PPI: Protein-protein interaction.

The results indicate that BP mainly involves positive regulation of gene expression, positive regulation of

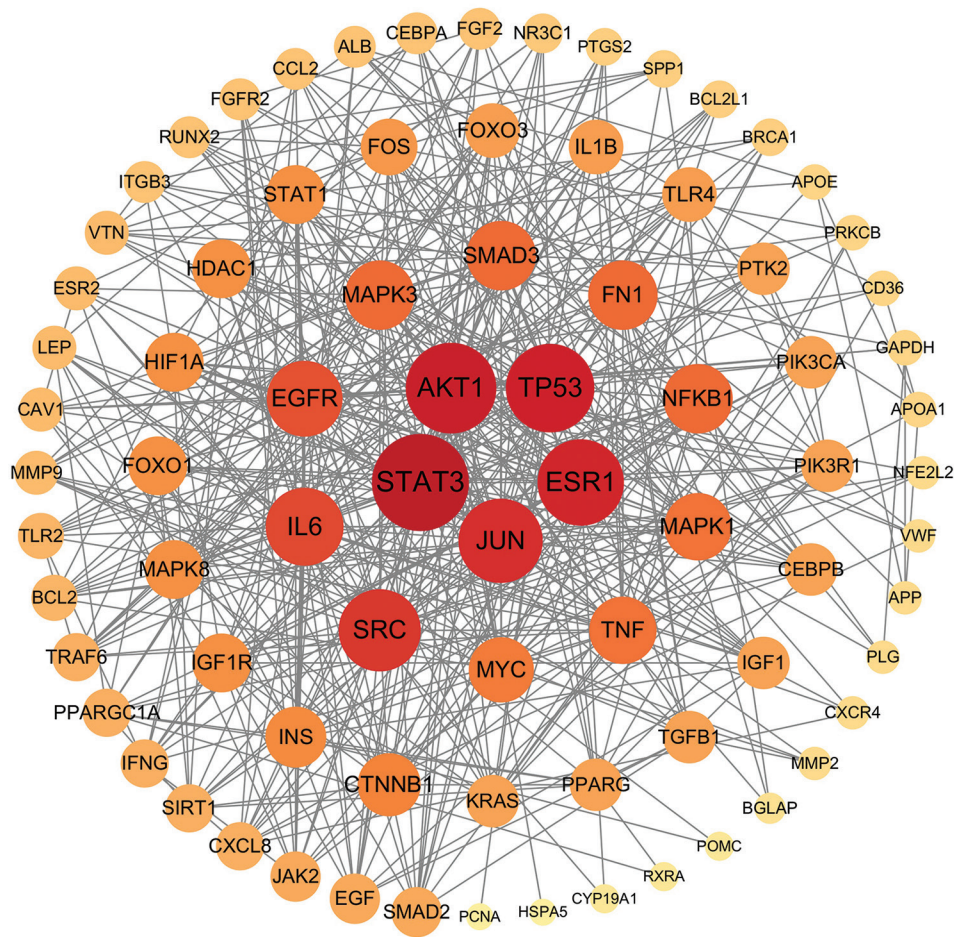


Figure 3. Core target network diagram involved in the treatment of OP using QGJSF
Abbreviations: OP: Osteoporosis; QGJSF: Qiang-gu-jian-shen formula.

RNA polymerase II transcription, positive regulation of DNA-templated transcription, response to exogenous stimulus, positive regulation of cell population proliferation, negative regulation of apoptotic processes, response to lipopolysaccharide, inflammatory response, response to hypoxia, and negative regulation of cell population proliferation. The CC is primarily associated with extracellular space, extracellular region, extracellular vesicle (exosome), cell surface, protein complex-containing structures, endoplasmic reticulum lumen, collagen-containing extracellular matrix, receptor complexes, plasma membrane side, and plasma membrane (cell membrane). The MF mainly concerns binding to identical proteins, enzyme binding, protein binding, nuclear receptor activity, signal receptor binding, DNA-binding transcription factor activity, cytokine activity, protein homodimerization activity, and RNA polymerase II-specific DNA-binding transcriptional activator activity.

KEGG pathway enrichment analysis predicts the role of protein target interaction networks in various cellular

activities and identifies key protein targets and their respective pathways. A total of 133 primary pathways were collected in the KEGG enrichment analysis. After excluding disease-named and cancer-related signaling pathways, the top 20 pathways were visualized using MicroSignal (Figure 5B). The enriched pathways are mainly involved in the PI3K/AKT signaling pathway, FoxO signaling pathway, HIF-1 signaling pathway, cellular senescence, osteoclast differentiation, TNF signaling pathway, Th17 cell differentiation, IL-17 signaling pathway, prolactin signaling pathway, and apoptosis signaling pathway.

3.7. Molecular docking

To investigate the interactions between the main active components of the potent bone-strengthening and kidney-nourishing formula and their corresponding core targets, molecular docking analysis was conducted using the AutoDock platform. The molecular structures of the compounds were downloaded from the PubChem database,

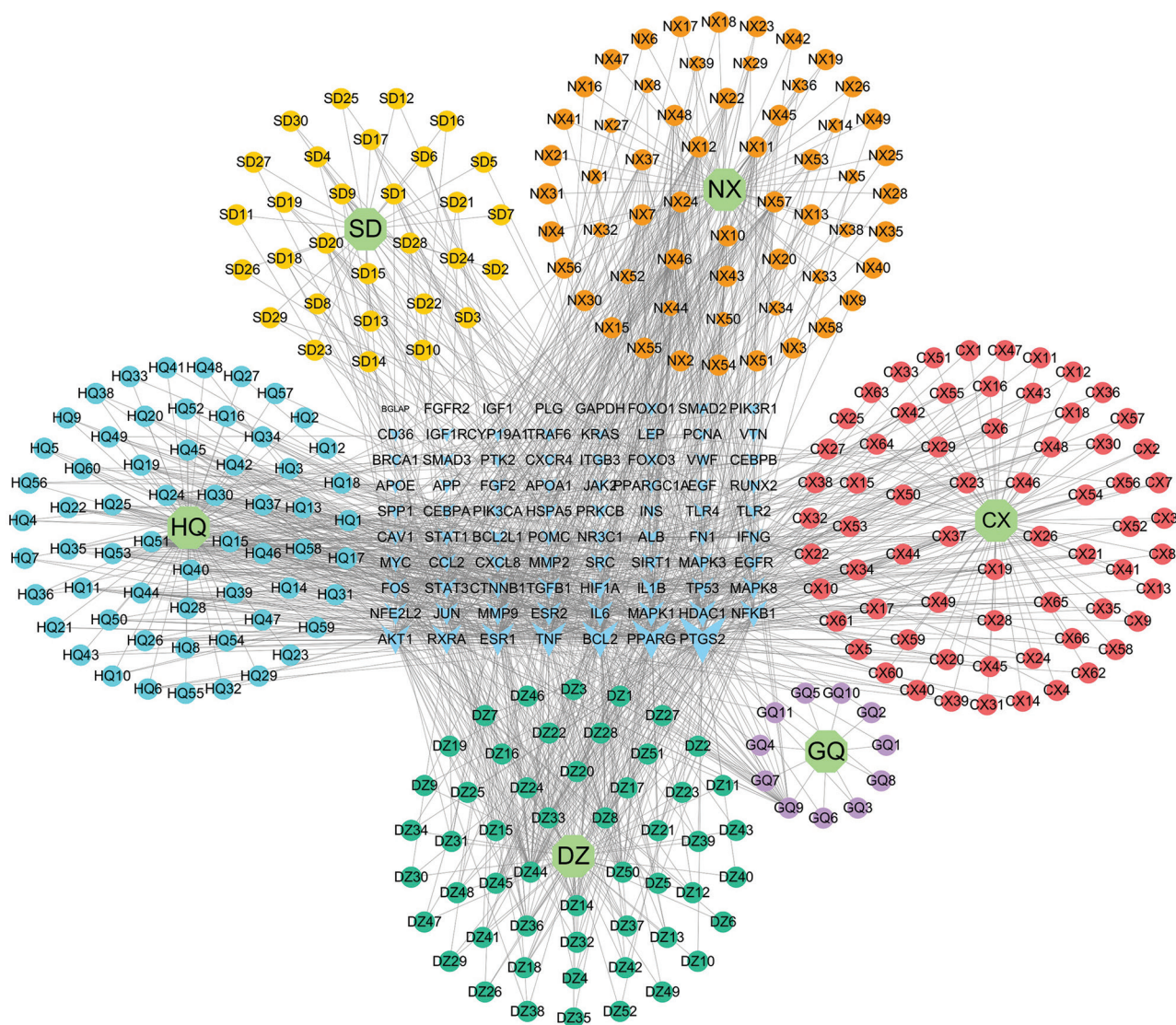


Figure 4. “Herb-active component-target” network diagram
Abbreviations: HQ: Huang Qi; DZ: Du Zhong; GQ: Gou Qi; NX: Niu Xi; SD: Shu Di; CX: Chuan Xiong.

and the 3D structures of the target proteins were obtained from the PDB. Protein receptors were pre-processed using PyMOL software to remove water molecules and existing ligands. Subsequently, the key components and target proteins were imported into AutoDockTools1.5.7 for hydrogen atom addition, active site, determination, and binding energy calculation.

In molecular docking analysis, a binding energy <math>< 0</math> kcal/mol indicates that the ligand can bind to the receptor spontaneously, without requiring external energy. A binding energy <math>< -5</math> kcal/mol suggests that the binding activity is favorable, indicating a strong affinity between the receptor and ligand (Figure 6).

Table 1. Key active components of the QGJSF

MolID	Chemical composition	Degree value	Belonging to TCMs
MOL000098	Quercetin	43	Cortex Eucommiae, Fructus Lycii, Radix Achyranthis Bidentatae, Radix Astragali
MOL002441	Dioscin	31	Radix Achyranthis Bidentatae
MOL000481	Genistein	28	Cortex Eucommiae
MOL000417	Calycosin	24	Radix Astragali
MOL001454	Berberine	24	Radix Achyranthis Bidentatae, Cortex Eucommiae

Abbreviations: QGJSF: Qiang-gu-jian-shen formula; TCMs: Traditional Chinese medicine.

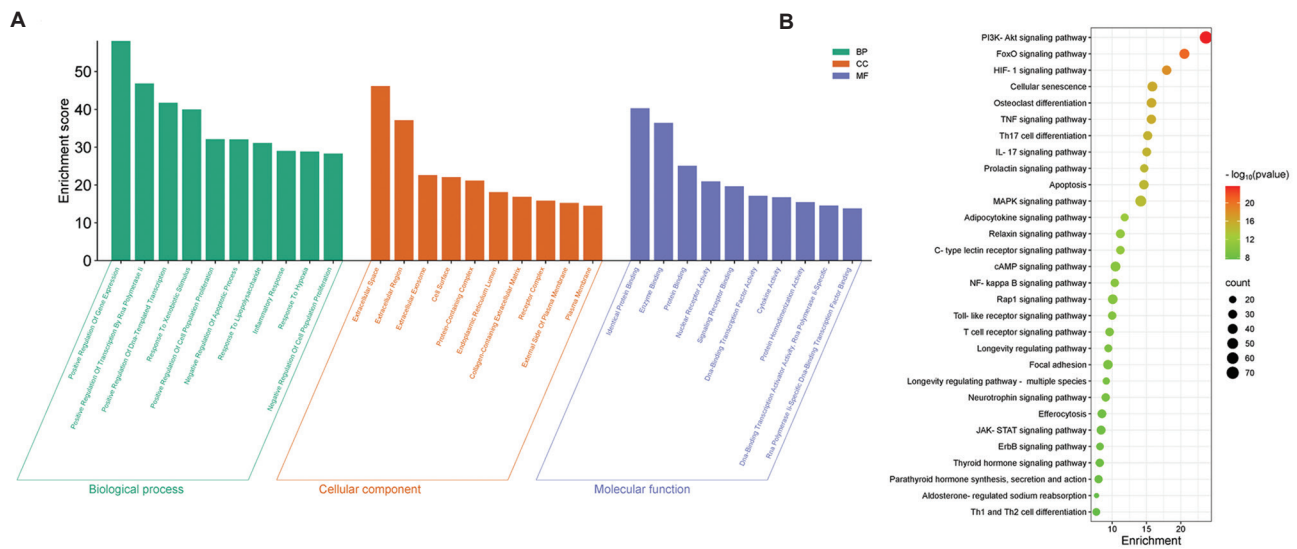


Figure 5. GO and KEGG Pathway Enrichment Analysis. (A) GO enrichment analysis. The top 10 terms of each category are displayed in a bar chart. (B) KEGG pathway enrichment analysis. The top 20 enriched pathways are displayed in a bubble chart. The bubble size indicates the number of genes enriched by the pathway, while bubble color intensity (redder color) indicates higher enrichment statistical significance (smaller corrected *p*-value). Abbreviations: GO: Gene ontology; KEGG: Kyoto encyclopedia of genes and genomes; BP: Biological process; CC: Cellular component; MF: Molecular function.

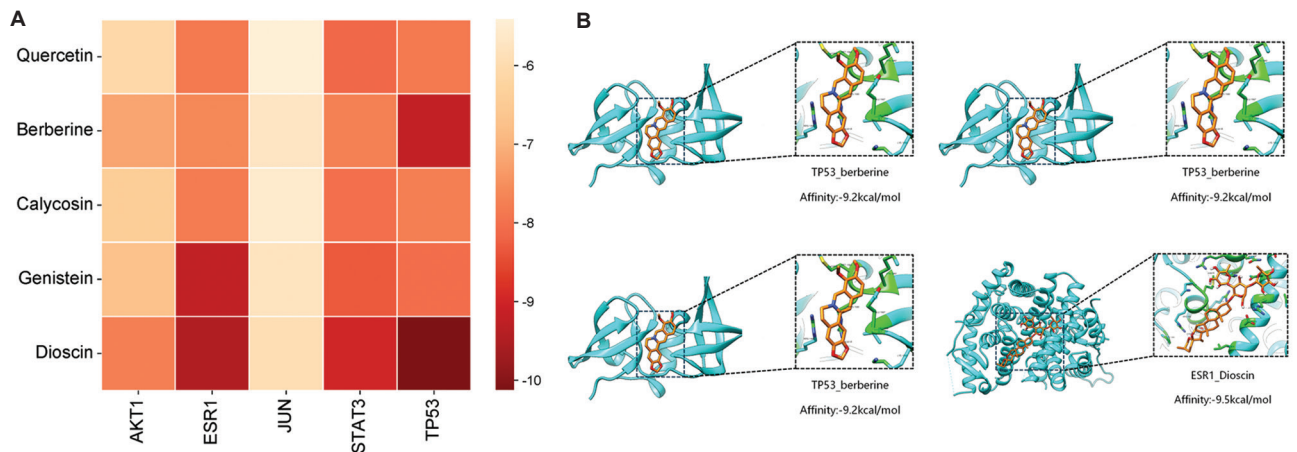


Figure 6. Molecular docking and visualization results. (A) Heatmap of binding energies from molecular docking. Darker colors represent lower binding energies. (B) Representative molecular docking interactions for four key component-target pairs. Abbreviations: AKT1: Protein kinase B; JUN: AP-1 transcription factor; STAT3: Signal transducer and activator of transcription 3; TP53: Tumor protein 53; ESR1: Estrogen receptor 1.

3.8. GEO database validation

To validate the potential targets identified in this study, differential expression analysis was conducted using the OP dataset GSE5958 from the GEO database. The “limma” R package was utilized to identify differentially expressed genes (DEGs) between control and osteoporotic samples. The number of DEGs was visualized using a volcano plot, where red dots represent upregulated genes, and blue dots represent downregulated genes. This graphical representation provides an overview of both the statistical

significance and fold changes in gene expression between the two groups. To further explore the expression patterns of the DEGs, a heatmap was constructed to visualize the distribution of the top 30 upregulated and top 30 downregulated genes across different sample groups. The heatmap offers a detailed look at the expression levels of these genes, highlighting the consistency or variability within and between the sample groups. After identifying the DEGs, a cross-referencing analysis was conducted to identify overlapping targets between the drugs used in

QGJSF and the DEGs from the GSE5958 dataset. This analysis led to the identification of seven shared core genes, such as TGFB1, MMP2, BCL2L1, MAPK3, AKT1, CTNNB1, and TP53 (Figure 7A-C). These genes serve as key points of intersection between the targets of QGJSF and the biological changes observed in OP, suggesting their critical role in the therapeutic effects of the formula.

3.9. Key gene expression validation

Next, the expression of the seven hub genes was validated in the GSE35958 dataset. The results showed that TGFB1, MMP2, BCL2L1, MAPK3, AKT1, and TP53 were significantly upregulated, while CTNNB1 was significantly downregulated in the OP group compared with normal control samples (Figure 8A-G).

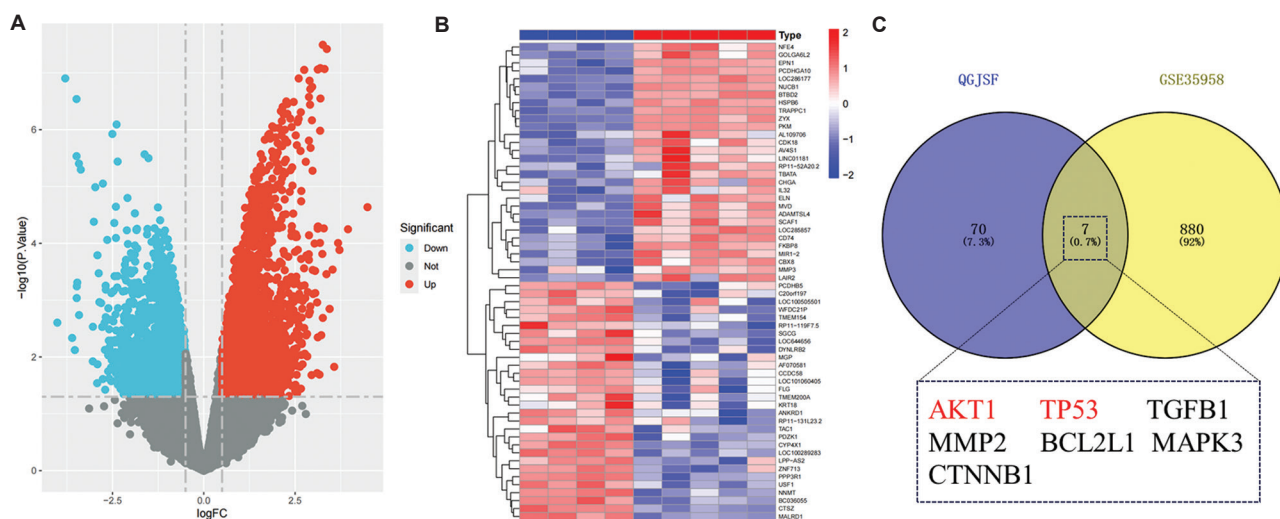


Figure 7. Validation of core targets of QGJSF using the GEO dataset (GSE35958). (A) Volcano plot of DEGs. (B) Heatmap of DEGs. (C) Venn analysis showing the overlap between QGJSF-associated genes and DEGs.

Abbreviations: DEGs: Differentially expressed genes; GEO: Gene expression omnibus; QGJSF: Qiang-gu-jian-shen formula.

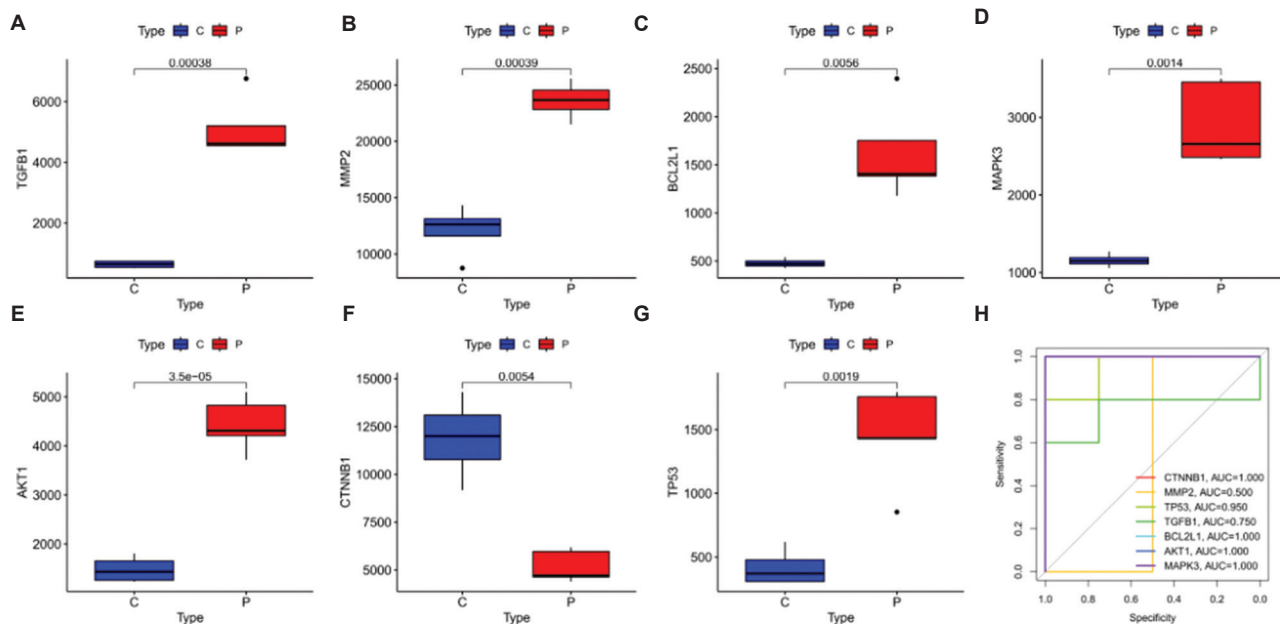


Figure 8. Validation of hub genes in GSE35958 dataset. (A-G) Expression levels of hub genes in GSE35958 dataset. (H) ROC curve analysis of hub genes in the GSE35958 dataset.

Abbreviations: C: Control; P: Osteoporosis; ROC: Receiver operating characteristic.

ROC curve analysis was then performed to explore the diagnostic effects of the seven hub genes. In the GSE35958 dataset, the area under the curve (AUC) values were as follows: TGFB1, AKT1, CTNNB1, and TP53 all had an AUC of 1.000, MMP2 was 0.500, BCL2L1 was 0.950, and MAPK3 was 0.750. Except for MMP2, all other genes had AUC values >0.7, suggesting good diagnostic performance (Figure 8H).

3.10. GSEA analysis

To explore the potential pathways of these six genes, single-gene GSEA analysis was performed. The results showed that the TGFB1 high-expression group was highly enriched in the pathways of autoimmune thyroid disease and ribosome (Figure 9A). The BCL2L1, MAPK3, and TP53 high-expression groups were highly enriched in the pathways of antigen processing and presentation, and autoimmune thyroid disease (Figure 9B). The AKT1 group was highly enriched in autoimmune thyroid disease and graft-versus-host disease (Figure 9C). Meanwhile, the CTNNB1 low-expression group was highly enriched in the ribosome and graft-versus-host disease pathways (Figure 9D).

4. Discussion

This study highlights the potential of QGJSF in treating OP through five key components, such as quercetin, dioscin, genistein, calycosin, and berberine, each targeting distinct molecular mechanisms. Quercetin promotes osteoblast differentiation and inhibits osteoclast activity through multiple pathways, including Wnt/ β -catenin, BMP/SMAD/RUNX2, OPG/RANKL/RANK, ERK/JNK, and GPRC6A/AMPK/mTOR, while modulating oxidative stress and metabolic regulation.^{8,9} Dioscin enhances bone formation in post-menopausal OP models by activating PI3K/P38/AKT signaling and suppressing TLR4/MyD88/TRAF6 pathways.^{10,11} Genistein, structurally similar to estrogen, mitigates bone marrow stem cell senescence

through $ERR\alpha$ -mediated mitochondrial biogenesis and regulates MAPK, NF- κ B, and NRF2/HO-1 pathways.^{12,13} Calycosin inhibits RANKL-induced osteoclastogenesis, upregulates OPG, and activates PI3K/AKT and Wnt/ β -catenin pathways to support osteoblast function and bone mineralization, while its antioxidant properties improve bone microstructure.¹⁴⁻¹⁶ Berberine reduces oxidative damage, suppresses RANKL/OPG signaling to inhibit osteoclasts, and promotes osteoblastogenesis through PKA, p38 MAPK, Wnt/ β -catenin, and AMPK pathways, enhancing bone strength and microarchitecture.¹⁷⁻²⁰ Collectively, these compounds regulate bone remodeling by balancing osteoblast and osteoclast activity, alleviating oxidative stress, and modulating key signaling pathways. Their synergistic effects may provide superior therapeutic outcomes for OP compared to monotherapy.

This study identified five core targets, such as STAT3, AKT1, TP53, ESR1, and JUN, through PPI network topology analysis, systematically revealing their multidimensional roles in bone metabolism regulation. These findings provide key insights into the pathogenesis of OP and the potential therapeutic targets of QGJSF.²¹ STAT3, a critical mediator of cytokine-kinase communication, exhibits bidirectional regulation of bone metabolism through the JAK-STAT pathway. It activates osteogenic genes, such as *Runx2*, *OCN*, *BSP*, *ALP*, and *COL1A1* to promote bone formation,^{21,22} while simultaneously binding to the NFATc1 promoter to drive osteoclast pre-cursor differentiation and regulate osteoclast-specific genes, such as osteoclast-associated receptor and dendrocyte expressed seven transmembrane protein (*Dc-Stamp*).^{23,24} In IL-6 family-mediated inflammatory responses, STAT3 suppresses RANKL signaling to alleviate bone loss, yet its abnormal activation exacerbates inflammatory bone destruction.²⁵ AKT1 activates the Wnt pathway by phosphorylating GSK3 β to stabilize β -catenin through the PI3K/AKT/mTOR axis, thereby promoting osteoblast differentiation

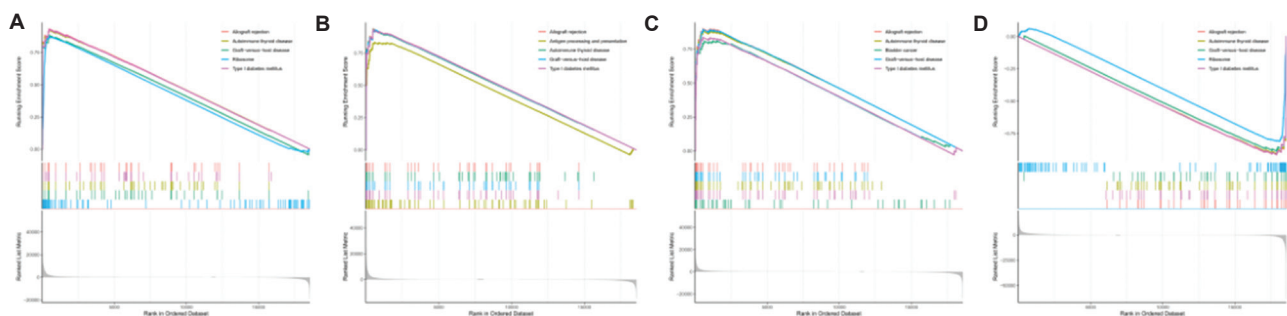


Figure 9. GSEA analysis of hub genes. (A) GSEA analysis of TGFB1. (B) GSEA analysis of BCL2L1, MAPK3, and TP53. (C) GSEA analysis of AKT1. (D) GSEA analysis of CTNNB1.

Abbreviations: GSEA: Gene set enrichment analysis; TGFB1: Transforming growth factor beta 1; MMP2: Matrix metalloproteinase 2; BCL2L1: BCL2 like 1; MAPK3: Mitogen-activated protein kinase 3; AKT1: AKT serine/threonine kinase 1; CTNNB1: Catenin beta 1.

and mineralization. Concurrently, it inhibits RANKL-induced osteoclast pre-cursor maturation, playing a dual regulatory role in maintaining the balance between bone formation and resorption.²⁶⁻²⁸ TP53, as a transcription factor, suppresses osteoblast differentiation by blocking OSX-DLX5 complex formation and inhibiting osteogenic gene expression (IBSP, COL1A1) while inducing pro-apoptotic genes (*NOXA*, *PUMA*). High-dose glucocorticoids activate the TP53 signaling pathway, downregulating OPG and upregulating RANKL to disrupt bone homeostasis; excessive TP53 activation further induces osteoclast cycle arrest and ferroptosis.²⁹⁻³⁶ ESR1 promotes BMSC osteogenic differentiation through the Wnt/ β -catenin, PI3K/AKT, and MAPK/ERK pathways. Its knockdown significantly reduces the expression of osteogenic markers (ALP, Runx2, OCN, OPN) and mineralized nodule formation. In gender-specific regulation, ESR1 primarily affects cortical bone in male mice and trabecular bone in female mice. In osteoclasts, ESR1 induces apoptosis through the FasL/Fas pathway to inhibit bone resorption and is regulated by SIRT6 in bone quality modulation.³⁷⁻⁴² JUN, a component of the AP-1 complex, activates late-stage osteoblast differentiation genes through the JNK signaling pathway and participates in cell proliferation, stress responses, and apoptosis to maintain osteocyte homeostasis.⁴³ In summary, STAT3, AKT1, TP53, ESR1, and JUN play pivotal roles in regulating bone metabolism, providing valuable insights into the pathophysiology of OP and highlighting potential therapeutic targets.

Enrichment analysis shows that the therapeutic mechanisms of QGJSF for OP involve the coordinated regulation of multiple signaling pathways. Under hypoxic conditions, HIF-1 α promotes osteoclast differentiation and glycolysis-mediated energy metabolism through ANGPTL4, while downstream VEGF enhances osteoclast activity through autocrine/paracrine pathways and mediates type H angiogenesis, directly linking bone mass regulation (HIF-1 α deficiency causes bone loss, whereas overexpression promotes vascular-osteogenic coupling).⁴⁴⁻⁴⁷ The FoxO pathway maintains redox homeostasis by activating antioxidant enzymes (e.g., SOD, Cat) and interacts with the Wnt/ β -catenin pathway: During aging, FoxO competes for β -catenin binding, inhibiting Wnt signaling, while JNK-mediated FoxO phosphorylation further disrupts β -catenin/TCF transcriptional activity, impairing osteoblast function.⁴⁸⁻⁵⁵ The PI3K/AKT pathway exhibits dual roles in bone metabolism: Activation promotes osteoblast differentiation (e.g., IL-37 enhances MSC osteogenesis and mineralization through this pathway⁵⁶), while M-CSF/RANKL-driven PI3K/AKT signaling fuels osteoclastogenesis, which can be suppressed by phytoestrogens (e.g., resveratrol) and

negative regulators, such as PTEN/SHIP.⁵⁷⁻⁶⁰ Aging-related pathways include p16/RB and p53/p21, which induce cell cycle arrest through DNA damage response and suppress osteogenesis (p53 inhibits Runx2/Osterix through miR-145 targeting Cbfb^{61,62}), while NF- κ B amplifies bone damage through SASP-mediated inflammatory cascades. Non-coding RNAs (e.g., lncRNA ZFAS1/miR-29a) epigenetically regulate Wnt/ β -catenin and FoxO pathways to influence bone homeostasis.^{63,64} The osteoclast differentiation network centers on the M-CSF/RANKL-RANK axis, activating NF- κ B/MAPK/NFATc1 signaling. STAT3 synergizes with c-fos to enhance NFATc1 activity, whereas OPG, miRNAs (e.g., miR-34a-5p), and lncRNAs (e.g., AK077216) modulate osteoclast-osteoblast balance in OP progression.⁶⁵⁻⁷¹ These pathways highlight molecular switches in OP pathogenesis, such as the HIF-1 α -VEGF axis in bone-vascular coupling and FoxO/Wnt crosstalk driving aging-related bone loss, and underscore therapeutic targets (e.g., PI3K/AKT plasticity, ncRNA-mediated epigenetic regulation) for precision interventions.

The integration of molecular docking results with network pharmacology and GEO validation analyses provides a multi-layered mechanistic explanation for the therapeutic effects of QGJSF in OP. Molecular docking studies revealed that key active components in QGJSF, including quercetin, dioscin, genistein, calycosin, and berberine, exhibit strong binding affinities to critical targets such as AKT1 and TP53, previously identified as core therapeutic hubs and validated in the GEO dataset (GSE35958). For instance, quercetin and calycosin showed stable interactions with AKT1, a central regulator of the PI3K/AKT pathway, potentially enhancing its activation to promote osteoblast survival and differentiation while suppressing osteoclastogenesis. Similarly, dioscin and baicalein demonstrated high binding potential with TP53, suggesting direct modulation of TP53-mediated apoptosis and cell cycle arrest, counteracting bone loss. Notably, these docking results align with the GEO findings where AKT1 and TP53 exhibited significant dysregulation (AUC = 1.000) in OP, reinforcing their roles as primary targets of QGJSF.

The identification of seven overlapping targets (including AKT1 and TP53) across the GEO dataset and QGJSF's core targets further bridges the gap between computational predictions and experimental validation. While STAT3, ESR1, and JUN also showed binding capabilities with QGJSF components, their lower diagnostic AUC values in GEO data compared to AKT1/TP53 suggest they may act as secondary or synergistic targets. This hierarchical target prioritization, with AKT1 and TP53 as the most diagnostically and mechanistically relevant,

supports the hypothesis that QGJSF exerts its anti-OP effects predominantly through stabilizing PI3K/AKT signaling (via AKT1 activation) and mitigating TP53-driven osteoblast apoptosis.

These findings collectively highlight a “multi-component, dual-core target” mechanism: QGJSF’s active ingredients physically engage AKT1 and TP53 to rectify their dysregulation in OP, while other targets (e.g., STAT3, CTNNB1) may contribute indirectly through pathway crosstalk or compensatory mechanisms. Future studies should prioritize *in vitro* validation of these docking interactions, for example by testing whether quercetin or dioscin modulates AKT1 phosphorylation or TP53 activity, to strengthen the translational relevance of these computational insights.

5. Conclusion

QGJSF potentially treats OP by acting through its components, quercetin, dioscin, genistein, calycosin, and berberine, on potential core targets such as STAT3, AKT1, TP53, ESR1, and JUN. These interactions modulate several signaling pathways including PI3K/AKT, FoxO, HIF-1, cellular senescence, and osteoclast differentiation. The formula intervenes in BP such as positive regulation of gene expression, RNA polymerase II transcription, cell proliferation, as well as negative regulation of apoptosis and cell proliferation. These molecular insights provide a theoretical basis for subsequent clinical and experimental studies on OP treatment. However, it is important to acknowledge the limitations of this study. The present analysis focuses solely on the direct relationships between QGJSF and OP-related components, targets, and pathways. Given that QGJSF is a TCM compound prescription, it may also improve the overall condition of OP patients by indirectly addressing pathological changes across multiple systems. This potential indirect therapeutic mechanism remains to be explored and elucidated further. The above findings provide valuable guidance for future research directions. Investigating the indirect effects of QGJSF on systemic health could offer additional strategies for treating OP and enhancing the quality of life for affected individuals. Moreover, understanding the comprehensive mechanisms of QGJSF will contribute to the development of more effective and personalized therapies for OP.

This study reveals potential molecular mechanisms by which QGJSF regulates bone metabolism through multi-dimensional analyses. Nonetheless, the synergistic effects of its components and dynamic regulatory mechanisms require further exploration. For instance, functional validation of core targets (e.g., AKT1, TP53) requires validation through gene-editing models to define their

regulatory thresholds, while the bidirectional effects of pathways such as PI3K/AKT may depend on component concentrations and microenvironmental factors, necessitating quantification using 3D bone organoids or dynamic culture systems. Future studies could integrate spatial transcriptomics and single-cell metabolomics to elucidate the spatiotemporal regulatory network of QGJSF in bone vascularization and oxidative stress microenvironments. In addition, combining clinical heterogeneity data to establish efficacy prediction models will advance precision intervention strategies for OP treatment using TCM formulations.

Acknowledgments

None.

Funding

None.

Conflict of interest

The authors declare they have no competing interests.

Author contributions

Conceptualization: Farra Aidah Jumuddin

Formal analysis: Zarina Awang

Investigation: Cuicui Zhou

Methodology: Cuicui Zhou, Farra Aidah Jumuddin

Writing – original draft: Cuicui Zhou

Writing – review & editing: Cuicui Zhou, Zarina Awang

Ethics approval and consent to participate

Not applicable.

Consent for publication

Not applicable.

Availability of data

Not applicable.

References

1. International Osteoporosis Foundation. *Worldwide Incidence of HIP Fracture Increase from 1990 to 2050 [EB/OL]*. Available from: <https://www.osteoporosisfoundation/policy-makers#policy-reports-audits> [Last accessed on 2025 Jun 16].
2. World Health Organization. *Musculoskeletal Conditions Affect Millions [EB/OL]*. Available from: <https://www.who.int/news/item/27-10-2003musculoskeletal-conditions-affect-millions> [Last accessed on 2025 Jun 16].
3. Schroeder RJ, Staszkiwicz J, O’Quin C, *et al.* Oral

- therapeutics post-menopausal osteoporosis. *Cureus*. 2023;15(8):e42870.
doi: 10.7759/cureus.42870
4. Wang L, Huang X, Qin J, *et al.* The role of traditional Chinese medicines in the treatment of osteoporosis. *Am J Chin Med*. 2024;52(4):949-986.
doi: 10.1142/S0192415X24500393
 5. Xiong M, Chen X, Wang H, *et al.* Combining transcriptomics and network pharmacology to reveal the mechanism of zuojin capsule improving spasmolytic polypeptide-expressing metaplasia. *J Ethnopharmacol*. 2024;318(Pt B):117075.
doi: 10.1016/j.jep.2023.117075
 6. Yu W, Li X, Sun Q, *et al.* Metabolomics and network pharmacology reveal the mechanism of *Castanopsis* honey against *Streptococcus pyogenes*. *Food Chem*. 2024;441:138388.
doi: 10.1016/j.foodchem.2024.138388
 7. Zhu H, Wang S, Shan C, *et al.* Mechanism of protective effect of xuan-bai-cheng-qi decoction on LPS-induced acute lung injury based on an integrated network pharmacology and RNA-sequencing approach. *Respir Res*. 2021;22(1):188.
doi: 10.1186/s12931-021-01781-1
 8. Deng TT, Ding WY, Lu XX, *et al.* Pharmacological and mechanistic aspects of quercetin in osteoporosis. *Front Pharmacol*. 2024;15:1338951.
doi: 10.3389/fphar.2024.1338951
 9. Xiong Y, Huang CW, Shi C, *et al.* Corrigendum: Quercetin suppresses ovariectomy-induced osteoporosis in rat mandibles by regulating autophagy and the NLRP3 pathway. *Exp Biol Med (Maywood)*. 2024;249:10149.
doi: 10.3389/ebm.2024.10149
 10. Wu S, Zhao F, Zhao J, *et al.* Dioscin improves postmenopausal osteoporosis through inducing bone formation and inhibiting apoptosis in ovariectomized rats. *Biosci Trends*. 2019;13(5):394-401.
doi: 10.5582/bst.2019.01186
 11. Tao X, Qi Y, Xu L, *et al.* Dioscin reduces ovariectomy-induced bone loss by enhancing osteoblastogenesis and inhibiting osteoclastogenesis *Pharmacol Res*. 2020;151:104397.
doi: 10.1016/j.phrs.2019.104397
 12. Li M, Yu Y, Xue K, *et al.* Genistein mitigates senescence of bone marrow mesenchymal stem cells via $ERR\alpha$ -mediated mitochondrial biogenesis and mitophagy in ovariectomized rats. *Redox Biol*. 2023;61:102649.
doi: 10.1016/j.redox.2023.102649
 13. Wu Z, Liu L. The protective activity of genistein against bone and cartilage diseases. *Front Pharmacol*. 2022;13:1016981.
doi: 10.3389/fphar.2022.1016981
 14. Quan GH, Wang H, Cao J, *et al.* Calycosin suppresses RANKL-mediated osteoclastogenesis through inhibition of MAPKs and NF- κ B. *Int J Mol Sci*. 2015;16(12):29496-29507.
doi: 10.3390/ijms161226179
 15. Li N, Tu Y, Shen Y, Qin Y, Lei C, Liu X. Calycosin attenuates osteoporosis and regulates the expression of OPG/RANKL in ovariectomized rats *via* MAPK signaling. *Pharmazie*. 2016;71(10):607-612.
doi: 10.1691/ph.2016.6627
 16. Duan X, Meng Q, Wang C, *et al.* Calycosin attenuates triglyceride accumulation and hepatic fibrosis in murine model of non-alcoholic steatohepatitis *via* activating farnesoid X receptor. *Phytomedicine*. 2017;25:83-92.
doi: 10.1016/j.phymed.2016.12.006
 17. Li Z, Geng YN, Jiang JD, Kong WJ. Antioxidant and anti-inflammatory activities of berberine in the treatment of diabetes mellitus. *Evid Based Complement Alternat Med*. 2014;2014:289264.
doi: 10.1155/2014/289264
 18. Lee JW, Mase N, Yonezawa T, *et al.* Palmatine attenuates osteoclast differentiation and function through inhibition of receptor activator of nuclear factor- κ B ligand expression in osteoblast cells. *Biol Pharm Bull*. 2010;33(10):1733-1739.
doi: 10.1248/bpb.33.1733
 19. Chen ZZ. Berberine induced apoptosis of human osteosarcoma cells by inhibiting phosphoinositide 3 kinase/protein kinase B (PI3K/Akt) signal pathway activation. *Iran J Public Health*. 2016;45(5):578-585.
 20. Li H, Miyahara T, Tezuka Y, Tran QL, Seto H, Kadota S. Effect of berberine on bone mineral density in SAMP6 as a senile osteoporosis model. *Biol Pharm Bull*. 2003;26(1):110-111.
doi: 10.1248/bpb.26.110
 21. Matsushita K, Itoh S, Ikeda S, Yamamoto Y, Yamauchi Y, Hayashi M. LIF/STAT3/SOCS3 signaling pathway in murine bone marrow stromal cells suppresses osteoblast differentiation. *J Cell Biochem*. 2014;115(7):1262-1268.
doi: 10.1002/jcb.24777
 22. Vimalraj S, Arumugam B, Miranda PJ, Selvamurugan N. Runx2: Structure, function, and phosphorylation in osteoblast differentiation. *Int J Biol Macromol*. 2015;78:202-208.
doi: 10.1016/j.ijbiomac.2015.04.008
 23. Wang L, Yang H, Huang J, *et al.* Targeted ptpn11 deletion in mice reveals the essential role of SHP2 in osteoblast differentiation and skeletal homeostasis. *Bone Res*. 2021;9(1):6.
doi: 10.1038/s41413-020-00129-7
 24. Zhou S, Dai Q, Huang X, *et al.* STAT3 is critical for

- skeletal development and bone homeostasis by regulating osteogenesis. *Nat Commun.* 2021;12(1):6891.
doi: 10.1038/s41467-021-27273-w
25. Joung YH, Darvin P, Kang DY, *et al.* Methylsulfonylmethane Inhibits RANKL-induced osteoclastogenesis in BMMs by suppressing NF- κ B and STAT3 activities. *PLoS One.* 2016;11(7):e0159891.
doi: 10.1371/journal.pone.0159891
 26. Zhang B, Qu Z, Hui H, *et al.* Exploring the therapeutic potential of isoorientin in the treatment of osteoporosis: A study using network pharmacology and experimental validation. *Mol Med.* 2024;30(1):27.
doi: 10.1186/s10020-024-00799-7
 27. Chen X, Chen W, Aung ZM, Han W, Zhang Y, Chai G. LY3023414 inhibits both osteogenesis and osteoclastogenesis through the PI3K/Akt/GSK3 signalling pathway. *Bone Joint Res.* 2021;10(4):237-249.
doi: 10.1302/2046-3758.104.BJR-2020-0255.R2
 28. Kawamura N, Kugimiya F, Oshima Y, *et al.* Akt1 in osteoblasts and osteoclasts controls bone remodeling. *PLoS One.* 2007;2(10):e1058.
doi: 10.1371/journal.pone.0001058
 29. Vaddavalli PL, Schumacher B. The p53 network: Cellular and systemic DNA damage responses in cancer and aging. *Trends Genet.* 2022;38(6):598-612.
doi: 10.1016/j.tig.2022.02.010
 30. Wang B, Wang J. Research progress on MDM2/MDMX heterodimer and MDMX phosphorylation in regulating p53. *Chin Bull Life Sci.* 2020;32(5):446-452.
doi: 10.13376/j.cblls/2020056
 31. Hojo H, Ohba S, He X, Lai LP, McMahon AP. Sp7/osterix is restricted to bone-forming vertebrates where it acts as a dlx co-factor in osteoblast specification. *Dev Cell.* 2016;37(3):238-253.
doi: 10.1016/j.devcel.2016.04.002
 32. Kawane T, Komori H, Liu W, *et al.* Dlx5 and mef2 regulate a novel runx2 enhancer for osteoblast-specific expression. *J Bone Miner Res.* 2014;29(9):1960-1969.
doi: 10.1002/jbmr.2240
 33. Zhen YF, Wang GD, Zhu LQ, *et al.* P53 dependent mitochondrial permeability transition pore opening is required for dexamethasone-induced death of osteoblasts. *J Cell Physiol.* 2014;229(10):1475-1483.
doi: 10.1002/jcp.24589
 34. Zhang F, Peng W, Zhang J, *et al.* P53 and Parkin co-regulate mitophagy in bone marrow mesenchymal stem cells to promote the repair of early steroid-induced osteonecrosis of the femoral head. *Cell Death Dis.* 2020;11(1):42.
doi: 10.1038/s41419-020-2238-1
 35. Zauli G, Rimondi E, Corallini F, Fadda R, Capitani S, Secchiero P. MDM2 antagonist nutlin-3 suppresses the proliferation and differentiation of human pre-osteoclasts through a p53-dependent pathway. *J Bone Miner Res.* 2007;22(10):1621-1630.
doi: 10.1359/jbmr.070618
 36. Tong X, Gu J, Chen M, *et al.* P53 positively regulates osteoprotegerin-mediated inhibition of osteoclastogenesis by downregulating TSC2-induced autophagy *in vitro.* *Differentiation.* 2020;114:58-66.
doi: 10.1016/j.diff.2020.06.002
 37. Qu L, Zhao M, Wang D, Song L, Zhou K. Research progress and mechanism of estrogen receptor α in postmenopausal osteoporosis. *Chin J Osteoporos.* 2024;30(7):1021-1027.
 38. Feng C, Xu Z, Tang X, Cao H, Zhang G, Tan J. Estrogen-related receptor α : A significant regulator and promising target in bone homeostasis and bone metastasis. *Molecules.* 2022;27(13):3976.
doi: 10.3390/molecules27133976
 39. Moon YJ, Zhang Z, Bang IH, *et al.* Sirtuin 6 in preosteoclasts suppresses age- and estrogen deficiency-related bone loss by stabilizing estrogen receptor α . *Cell Death Differ.* 2019;26(11):2358-2370.
doi: 10.1038/s41418-019-0306-9
 40. Kim SJ, Piao Y, Lee MG, *et al.* Loss of sirtuin 6 in osteoblast lineage cells activates osteoclasts, resulting in osteopenia. *Bone.* 2020;138:115497.
doi: 10.1016/j.bone.2020.115497
 41. Melville KM, Kelly NH, Surita G, *et al.* Effects of deletion of ER α in osteoblast-lineage cells on bone mass and adaptation to mechanical loading differ in female and male mice. *J Bone Miner Res.* 2015;30(8):1468-1480.
doi: 10.1002/jbmr.2488
 42. Yang Y, Feng N, Liang L, *et al.* Progranulin, a moderator of estrogen/estrogen receptor α binding, regulates bone homeostasis through PERK/p-eIF2 signaling pathway. *J Mol Med (Berl).* 2022;100(8):1191-1207.
doi: 10.1007/s00109-022-02233-z
 43. León-Reyes G, Argoty-Pantoja AD, Becerra-Cervera A, López-Montoya P, Rivera-Paredes B, Velázquez-Cruz R. Oxidative-stress-related genes in osteoporosis: A systematic review. *Antioxidants (Basel).* 2023;12(4):915.
doi: 10.3390/antiox12040915
 44. Knowles HJ, Cleton-Jansen AM, Korsching E, Athanasou NA. Hypoxia-inducible factor regulates osteoclast-mediated bone resorption: Role of angiotensin-like 4. *FASEB J.* 2010;24(12):4648-4659.

- doi: 10.1096/fj.10-162230
45. Yao Z, Getting SJ, Locke IC. Regulation of TNF-induced osteoclast differentiation. *Cells*. 2021;11(1):132.
doi: 10.3390/cells11010132
 46. Miyauchi Y, Sato Y, Kobayashi T, *et al.* HIF1 α is required for osteoclast activation by estrogen deficiency in postmenopausal osteoporosis. *Proc Natl Acad Sci U S A*. 2013;110(41):16568-16573.
doi: 10.1073/pnas.1308755110
 47. Wan C, Shao J, Gilbert SR, *et al.* Role of HIF-1 α in skeletal development. *Ann N Y Acad Sci*. 2010;1192:322-326.
doi: 10.1111/j.1749-6632.2009.05238.x
 48. Medema RH, Kops GJ, Bos JL, Burgering BM. AFX-like forkhead transcription factors mediate cell-cycle regulation by ras and PKB through p27kip1. *Nature*. 2000;404(6779):782-787.
doi: 10.1038/35008115
 49. Tran H, Brunet A, Grenier JM, *et al.* DNA repair pathway stimulated by the forkhead transcription factor FOXO3a through the gadd45 protein. *Science*. 2002;296(5567):530-534.
doi: 10.1126/science.1068712
 50. Kops GJ, Dansen TB, Polderman PE, *et al.* Forkhead transcription factor FOXO3a protects quiescent cells from oxidative stress. *Nature*. 2002;419(6904):316-321.
doi: 10.1038/nature01036
 51. Brunet A, Bonni A, Zigmund MJ, *et al.* Akt promotes cell survival by phosphorylating and inhibiting a forkhead transcription factor. *Cell*. 1999;96(6):857-868.
doi: 10.1016/s0092-8674(00)80595-4
 52. Nemoto S, Finkel T. Redox regulation of forkhead proteins through a p66shc-dependent signaling pathway. *Science*. 2002;295(5564):2450-2452.
doi: 10.1126/science.1069004
 53. Speckmann B, Walter PL, Alili L, *et al.* Selenoprotein P expression is controlled through interaction of the coactivator PGC-1 α with FoxO1a and hepatocyte nuclear factor 4 α transcription factors. *Hepatology*. 2008;48(6):1998-2006.
doi: 10.1002/hep.22526.
 54. Sidhu A, Miller PJ, Hollenbach AD. FOXO1 stimulates ceruloplasmin promoter activity in human hepatoma cells treated with IL-6. *Biochem Biophys Res Commun*. 2011;404(4):963-967.
doi: 10.1016/j.bbrc.2010.12.089
 55. Almeida M. Unraveling the role of FoxOs in bone-insights from mouse models. *Bone*. 2011;49(3):319-327.
doi: 10.1016/j.bone.2011.05.023
 56. Y Ye C, Zhang W, Hang K, *et al.* Extracellular IL-37 promotes osteogenic differentiation of human bone marrow mesenchymal stem cells via activation of the PI3K/AKT signaling pathway. *Cell Death Dis*. 2019;10(10):753.
doi: 10.1038/s41419-019-1904-7
 57. Zhou H, Jiao G, Dong M, *et al.* Orthosilicic acid accelerates bone formation in human osteoblast-like cells through the PI3K-Akt-mTOR pathway. *Biol Trace Elem Res*. 2019;190(2):327-335.
doi: 10.1007/s12011-018-1574-9
 58. Bartell SM, Kim HN, Ambrogini E, *et al.* FoxO proteins restrain osteoclastogenesis and bone resorption by attenuating H₂O₂ accumulation. *Nat Commun*. 2014;5:3773.
doi: 10.1038/ncomms4773
 59. Feng Y. *Ph.D. Thesis*. China: Lanzhou University; 2018.
 60. Sugatani T, Alvarez U, Hruska KA. PTEN regulates RANKL- and osteopontin-stimulated signal transduction during osteoclast differentiation and cell motility. *J Biol Chem*. 2003;278(7):5001-5008.
doi: 10.1074/jbc.M209299200
 61. Stein GH, Drullinger LF, Soulard A, Dulić V. Differential roles for cyclin-dependent kinase inhibitors p21 and p16 in the mechanisms of senescence and differentiation in human fibroblasts. *Mol Cell Biol*. 1999;19(3):2109-2117.
doi: 10.1128/MCB.19.3.2109
 62. Xia C, Jiang T, Wang Y, Chen X, Hu Y, Gao Y. The p53/miR-145a axis promotes cellular senescence and inhibits osteogenic differentiation by targeting cbfb in mesenchymal stem cells. *Front Endocrinol (Lausanne)*. 2021;11:609186.
doi: 10.3389/fendo.2020.609186
 63. Kim HJ, Kim WJ, Shin HR, *et al.* ROS-induced PADI2 downregulation accelerates cellular senescence via the stimulation of SASP production and NF κ B activation. *Cell Mol Life Sci*. 2022;79(3):155.
doi: 10.1007/s00018-022-04186-5
 64. Lian WS, Wu RW, Chen YS, *et al.* MicroRNA-29a mitigates osteoblast senescence and counteracts bone loss through oxidation resistance-1 Control of FoxO3 methylation. *Antioxidants (Basel)*. 2021;10(8):1248.
doi: 10.3390/antiox10081248
 65. Raynaud-Messina B, Verollet C, Maridonneau-Parini I. The osteoclast, a target cell for microorganisms. *Bone*. 2019;127:315-323.
doi: 10.1016/j.bone.2019.06.023
 66. Tokunaga T, Mokuda S, Kohno H, *et al.* TGF β 1 regulates human RANKL-induced osteoclastogenesis via suppression of NFATc1 expression. *Int J Mol Sci*. 2020;21(3):800.

- doi: 10.3390/ijms21030800
67. Hu F, Jiang C, Bu G, Fu Y, Yu Y. Silencing long noncoding RNA colon cancer-associated transcript-1 upregulates microRNA-34a-5p to promote proliferation and differentiation of osteoblasts in osteoporosis. *Cancer Gene Ther.* 2021;28(10-11):1150-1161.
doi: 10.1038/s41417-020-00264-7
68. John AA, Xie J, Yang YS, *et al.* AAV-mediated delivery of osteoblast/osteoclast-regulating miRNAs for osteoporosis therapy. *Mol Ther Nucleic Acids.* 2022;29:296-311.
doi: 10.1016/j.omtn.2022.07.008
69. Li D, Liu J, Guo B, *et al.* Osteoclast-derived exosomal miR-214-3p inhibits osteoblastic bone formation. *Nat Commun.* 2016;7:10872.
doi: 10.1038/ncomms10872
70. Ohnuma K, Kasagi S, Uto K, *et al.* MicroRNA-124 inhibits TNF- α - and IL-6-induced osteoclastogenesis. *Rheumatol Int.* 2019;39(4):689-695.
doi: 10.1007/s00296-018-4218-7
71. Liu C, Cao Z, Bai Y, *et al.* LncRNA AK077216 promotes RANKL-induced osteoclastogenesis and bone resorption via NFATc1 by inhibition of NIP45. *J Cell Physiol.* 2019;234(2):1606-1617.
doi: 10.1002/jcp.27031